International Journal of Occupational Safety and Ergonomics (*JOSE*) 2005, Vol. 11, No. 2, 211–215

NOTES

Investigations of Single and Multilayer Structures Using Lock-In Thermography—Possible Applications

Grzegorz Gralewicz
Grzegorz Owczarek

Department of Personal Protective Equipment, Central Institute for Labour Protection – National Research Institute, Łódź, Poland

Bogusław Więcek

Institute of Electronics, Technical University of Łódź, Łódź, Poland

This paper presents a study of the possibilities of evaluating thermal parameters of single and multilayer structures using dynamic thermography. It also discusses potential uses of lock-in thermography. It presents a simulation of a periodic excitation of a multilayer composite material. In practice, the described methods can be employed in various applications, for example, in multilayer nonwoven microelectronic components manufactured from hemp fibers, chemical fibers, with an addition of electrically conducting fibers, and in medicine and biology.

This paper describes tests conducted with lock-in thermography on carbon fibre reinforced composites with implanted delamination defects. Lock-in thermography is a versatile tool for non-destructive evaluation (NDE). Lock-in thermography is a fast, remote and non-destructive procedure. Hence, it has been used to detect delaminations in the composite structure of aircraft. This method directly contributes to an improvement in safety.

lock-in and pulse thermography NDT transient state thermal modelling
effusivity and diffusivity

1. INTRODUCTION

Carbon fibre composites are now fairly widely used in civilian and military aircraft structures. Delaminations are common defects found in these materials. Their presence leads to structural weaknesses, which cause failure of airframe structures. It is important to develop effective non-destructive testing procedures to identify these defects and to increase the safety of aircraft travel.

Active thermography can be successfully employed in thermal investigations of both multilayer and thin film materials [1, 2, 3, 4, 5, 6, 7, 8, 9]. In microelectronics the multilayer structures of thin films are found in many semiconductor devices, e.g., power transistors containing joints between molybdenum substrates and silicon wafers. Thermal properties of thin films play an important role in dissipating power.

We propose a new method of measuring thermal conductivity and the thickness of thin layers, also

Correspondence and requests for offprints should be sent to Grzegorz Gralewicz, Central Institute for Labour Protection – National Research Institute, ul. Wierzbowa 48, 90-133 Łódź, Poland. E-mail: <grgra@ciop.lodz.pl>

applicable in multilayer structures. We measured the surface of this distribution in a very thick material measured in the range of micrometers. We calculated the phase of the thermal response and correlate it with thickness and thermal conductivity. The modelling results were compared with the measurements. To verify the correctness of the proposed approach we conducted tests on multilayer structures of different thickness. The presented methods and apparatus can be used for testing thermal properties of materials in microelectronics as well as in medicine and biology, e.g., to measure the thickness of skin layers.

2. THERMAL MODEL OF MULTILAYER STRUCTURE—PERIODIC EXCITATION

Let us consider a multilayer structure of the thickness L as shown in Figure 1. As an exemplary structure to verify the correctness of the approach we considered thin films of teflon and epoxy placed in a carbon-fibre-reinforced polymer (CFRP) [5].

Periodically varying heat flux is delivered to the upper side of the sample, where convection is defined to get real conditions of energy dissipation to the ambient. A 1-D model of the heat transfer in the solid is expressed as:

$$\frac{\partial^2 T}{\partial^2 x} - \frac{\rho c}{\lambda}\frac{\partial T}{\partial t} = 0 \tag{1}$$

with the boundary conditions represented by convective heat transfer coefficients h_f at the upper and h_r bottom side of the sample:

$$-\lambda\frac{\partial T}{\partial x} = \frac{Q_0}{2}\left[1+\cos(\omega t)\right] - h_{\mathrm{f}}\left(T_{\mathrm{f}} - T_\infty\right), \tag{2}$$

$$-k\frac{\partial T}{\partial x} = h_{\mathrm{r}}\left(T_{\mathrm{r}} - T_\infty\right). \tag{3}$$

An analytical solution of Equation 1 consists of dc (T_d) and ac (T_a) components of temperature [5].

$$T(x,t) = T_d(x) + T_a(x)\exp(j\omega t). \tag{4}$$

By placing Equation 4 in Equation 1 we can get the following result:

$$\exp(j\omega t)\left(\frac{d^2 T_a(x)}{d^2 x} - j\omega\frac{\rho c}{\lambda}T_a(x)\right) = 0, \tag{5}$$

with the boundary conditions which are expressed as:

$$-k\frac{dT_a(x)}{dx} = \frac{Q_0}{2} - h_{\mathrm{f}}T_{a\mathrm{f}} \qquad x = 0, \tag{6}$$

$$-k\frac{dT_a(x)}{dx} = h_{\mathrm{r}}T_{a\mathrm{r}} \qquad x = L. \tag{7}$$

The general solution of Equation 1 takes the form:

$$T_a(x) = A\exp(-\sigma x) + B\exp(\sigma x), \tag{8}$$

where $\sigma = (1+j)\left(\frac{\omega}{2\alpha}\right)^{1/2}$.

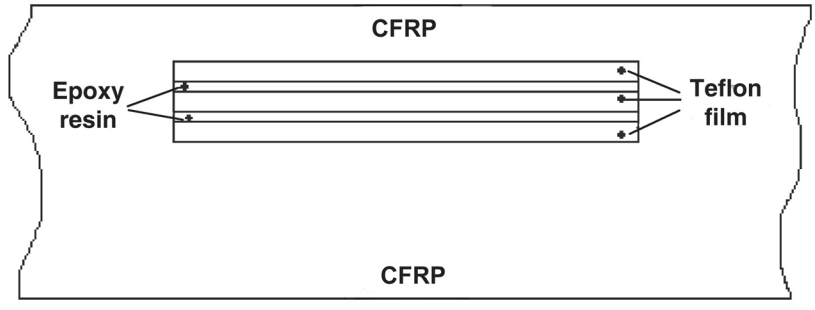

Figure 1. Multilayer structure. *Notes.* CFRP—carbon-fibre-reinforced-polymer.

TABLE 1. Material Constants Used for Simulations

Material	Density (kg m^{-3})	Thermal Conductivity (W m^{-1} °K^{-1})	Specific Heat (kJ kg^{-1} °K^{-1})
CFRP	1,600	0.670	1.200
Teflon	2,150	0.209	1.100
Epoxy resin	1,300	0.200	1.700

Notes. CFRP—carbon-fibre-reinforced polymer.

For a single layer structure the unknown constants A and B can be obtained using previously defined boundary conditions, which leads to the final set of equations.

$$\begin{cases} A(k_1\sigma_1 + h_f) + B(-k_1\sigma_1 + h_f) = \dfrac{Q_0}{2} \\ A(k_1\sigma_1 - h_r)\exp(-2\sigma_1 L) \\ \quad + B(-k_1\sigma_1 - h_r)\exp(2\sigma_1 L) = 0. \end{cases} \tag{9}$$

At the upper side, for $x = 0$, where the flux heats up the sample, temperature is simply expressed as:

$$T_a(0) = A + B, \tag{10}$$

and the phase can be derived from the equation.

$$\Phi = ArgT_a(0). \tag{11}$$

For a multilayer structure with n layers a similar approach is applied for every layer.

$$\frac{\partial^2 T_i}{\partial^2 x} - \frac{\rho_i c_i}{\lambda_i}\frac{\partial T_i}{\partial t} = 0 \qquad x_i \geq x \geq x_{(i-1)}$$
$$i = 1,...,n. \tag{12}$$

At each interface between the layers, temperature is continuous and the same heat flux is on both sides of the layer as there is no leakage of energy inside the sample.

$$\lambda_i \frac{\partial T_i}{\partial x} = \lambda_{(i+1)} \frac{\partial T_{(i+1)}}{\partial x} \qquad x = x_i,\ i = 1,...,n-1. \tag{13}$$

The interface is characterized by its thermal resistance $R_{i,i+1}$ and

$$T_{(i+1)} - T_i = R_{i,i+1}\lambda_{(i+1)}\frac{\partial T_{(i+1)}}{\partial x} \quad x = x_i,\ i = 1,...,n-1. \tag{14}$$

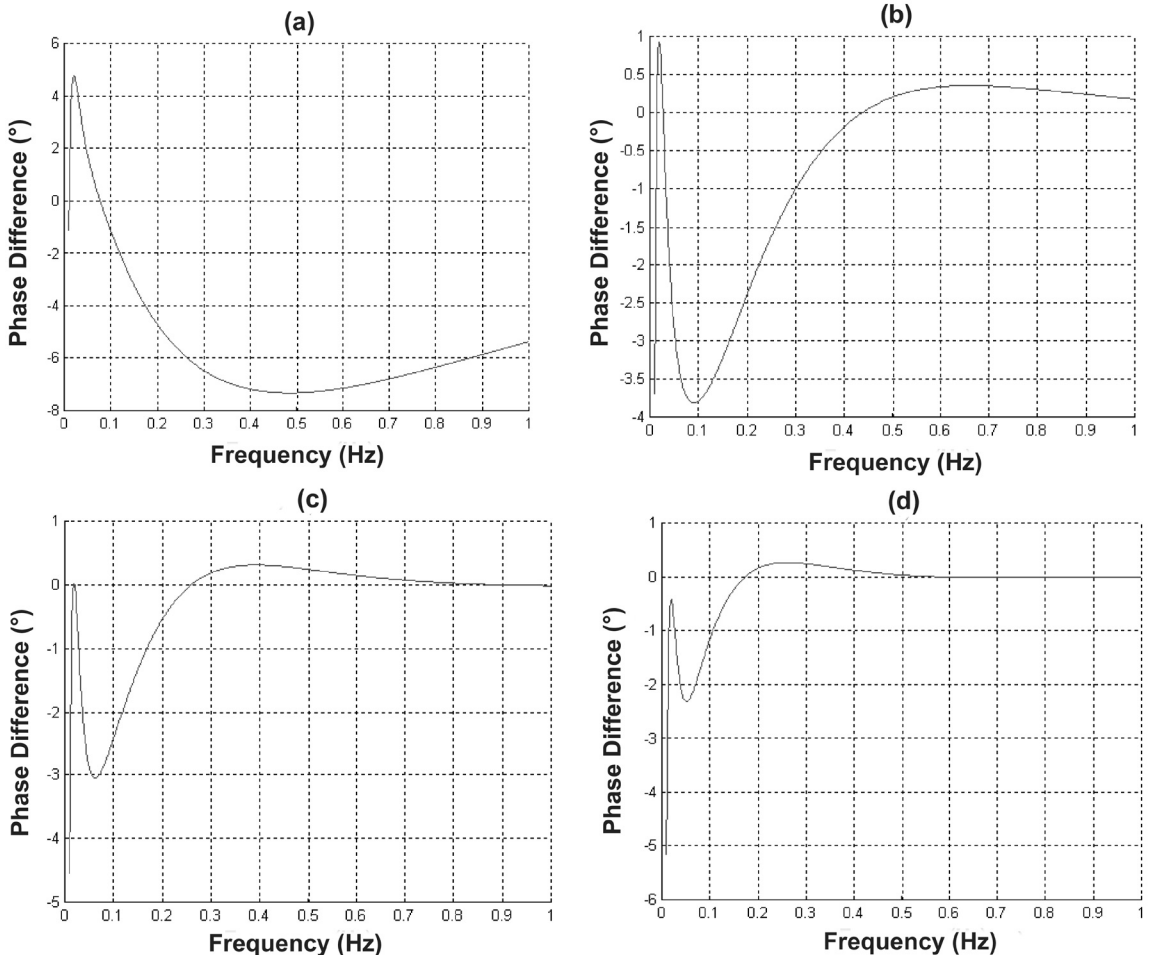

Figure 2. Phase differences between defective and homogenous areas for an 11-mm thickness of a defect, and its depths of (a) 0.28 mm, (b) 0.56 mm, (c) 0.84 mm and (d) 1.12 mm.

As before, for the upper and lower layer convective boundary conditions are applied:

$$\begin{aligned} -\lambda_1 \frac{\partial T_1}{\partial x} &= \frac{Q_0}{2}\left[1+\cos(\omega t)\right] - h_{\mathrm{f}}\left(T_{\mathrm{f}} - T_\infty\right) \\ -\lambda_n \frac{\partial T_n}{\partial x} &= h_{\mathrm{r}}\left(T_{\mathrm{r}} - T_\infty\right). \end{aligned} \tag{15}$$

By separating the analytical solution for the dc and ac components, we get a solution for each layer.

$$T_{ai}(x) = A_i \exp(-\sigma_i x) + B_i \exp(\sigma_i x), \tag{16}$$

with unknown constants A_i, B_i

and $\sigma_i = (1+j)\left(\frac{\omega}{2\alpha_i}\right)^{1/2}$.

The final set of linear equations takes the form:

$$\begin{cases} A_1\left(k_1\sigma_1 + h_f\right) + B_1\left(-k_1\sigma_1 - h_{\mathrm{f}}\right) = \dfrac{Q_0}{2} \\ A_i\left(-k_i\sigma_i \exp(-\sigma_i x_i)\right) + B_i\left(k_i\sigma_i \exp(\sigma_i x_i)\right) + A_{(i+1)}\left(k_{(i+1)}\sigma_{(i+1)} \exp\left(-\sigma_{(i+1)}x_i\right)\right) \\ + B_{(i+1)}\left(-k_{(i+1)}\sigma_{(i+1)} \exp\left(\sigma_{(i+1)}x_i\right)\right) = 0 \\ A_i\left(-\exp(-\sigma_i x_i)\right) + B_i\left(-\exp(\sigma_i x_i)\right) + A_{(i+1)}\left(\left(1+R_{i,i+1}k_{(i+1)}\sigma_{(i+1)}\right)\exp\left(-\sigma_{(i+1)}x_i\right)\right) \\ + B_{(i+1)}\left(\left(1-R_{i,i+1}k_{(i+1)}\sigma_{(i+1)}\right)\exp\left(\sigma_{(i+1)}x_i\right)\right) = 0 \\ A_n\left(k_n\sigma_n - h_r\right)\exp(-\sigma_n x_n) + B_n\left(-k_n\sigma_n - h_{\mathrm{r}}\right)\exp(\sigma_n x_n) = 0. \end{cases} \tag{17}$$

At the upper side of the sample, the amplitude and phase of the ac component of temperature can be easily calculated as $T_{af} = A_1 + B_1$, $\Phi = Arg(A_1 + B_1)$.

Finally, the phase difference of the temperature between for the place where the defect is, and for homogenous material is calculated as Equation 5:

$$\Delta\Phi = \Phi_{\mathrm{defect}} - \Phi_{\mathrm{homogenous}} \tag{18}$$

Simulations were performed for different depths of the defect with different material constants (Figure 2).

3. CONCLUSION

Lock-in thermography is one of the most promising methods for dynamic process investigations for possible use in many technical and medical applications. Heat transfer modelling proves the method potential for defect and multilayer structure measurements. The results obtained in this study confirm the thesis that lock-in thermography methods are very useful in evaluating thermal and geometrical properties of single and multilayer materials. Using temperature decay during cooling down processes, or from the measurment phase difference, we can nominate materials with different thermal properties, such as thermal conductivity and diffusivity. Thermography investigations should be performed very carefully to reduce interference from elements with a significant influence on the result, e.g., infrared reflection, non-stable conditions, undefined convective heat transfer coefficient.

In practical inspections, one should try to use optimum frequencies. A one-dimensional photothermal model can approximately predict the result of the inspection. The model is very valuable for selecting inspection parameters, which should result in great cost savings. More work on the use of active thermography is planned in field of improving safety in everyday life and work.

SYMBOLS

Symbol	Explanation
L	Thickness
Q_0	Intensity of the heat source
ω	Angular modulation frequency
t	Time
k	Thermal conductivity
ρ	Density
c_{w}	Specific heat
x	Perpendicular distance from the front surface
T	Temperature
T_{f}	Temperature of the front surface
T_{r}	Temperature of the rear surface

T_∞	Ambient temperature
h_f	Surface heat transfer coefficient of the front surface
h_r	Surface heat transfer coefficient of the rear surface
T_d	dc (constant) component of the temperature
T_a	ac (variable) component of the temperature
T_{df}	Spatial dependence of the dc temperature component for the front surface
T_{dr}	Spatial dependence of the dc temperature component for the front surface
T_{af}	Spatial dependence of the ac temperature component for the front surface
T_{ar}	Spatial dependence of the ac temperature component for the rear surface
Φ	Phase difference between the surface temperature and the heat source
$R_{i,i+1}$	Thermal contact resistance between medium i and medium $i + 1$
$\Delta\Phi$	Phase difference between the defective and the non-defective area
$\Phi_{\text{non–defective}}$	Phase of the non-defective area
$\Phi_{\text{defective}}$	Phase of the defective area
α	Thermal diffusivity

REFERENCES

1. Almond DP, Patel PM. Photothermal science and techniques. London, UK; Chapman & Hall; 1996.
2. Almond DP, Lau C K. Defect sizing by transient thermography, an analytical treatment. J Phys D: Appl Phys 194;27:1063–9.
3. Krapez J-C. Compared performances of four algorithms used for digital lock-in thermography. In: Proceedings of the Eurotherm Seminar 60: Quantitative Infrared Thermography 4—QIRT '98, September 7–10, 1998, Łódź, Poland. Retrieved July 15, 2004, from: http://www.onera.fr/SEARCH/BASIS/public/web_en/document/DDD/301679.pdf
4. Netzelmann U, Walle G. High-speed pulsed thermography of thin metallic coatings. In: Proceedings of the Eurotherm Seminar 60 Quantitative Infrared Thermography–QIRT '98, September 7–10, 1998, Łódź, Poland, p. 81–5.
5. Bai W, Wong BS. Evaluation of defects in composite plates under convective environments using lock-in thermography. Measurements Science and Technology 2001;12:142–50.
6. Almond D, Busse G, Grinzato E, Krapez JC, Maldague X, Vavilov V, et al. Infrared thermographic detection and characterisation of impact damage in carbon fibre composites: results of the round robin test. In: Proceedings of the Eurotherm Seminar 60 Quantitative Infrared Thermography—QIRT '98, September 7–10, 1998, Łódź, Poland, p. 43–52.
7. Krucińska I, Michalak M. Barrier properties of textiles with hemp fiber components. In: Włókiennictwo: 2nd international conference, MTE 2000, Metrology in Textile Engineering. 1st international workshop, NETECOFLAX-2000, Ecological high quality cottonized flax fabrics production from worthless raw material, November 23–24, 2000, Łódź, Poland (Zeszyty Naukowe, No. 855). Łódź, Poland: Wydawnictwo Politechniki Łódzkiej; 2000.
8. Michalak M, Krucińska I, Więcek B. Application of thermography for slow and fast varying thermal processes in textile research In: Proceedings of Eurotherm Seminar No. 64, Reims, France, July 18–21, 2000. p. 283–8.
9. Więcek B, Zwolenik S. Thermal wave method—limits and potentialities of active thermography in biology and medicine. In: 2nd Joint EMBS-BMES Conference, 24th Annual International Conference of the IEEE Engineering in Medicine and Biology Society, BMES-EMS 2002, Houston, TX, USA, October 23–26, 2002.